C.P. No. 1310

C.P. No. 1310

PROCUREMENT EXECUTIVE, MINISTRY OF DEFENCE

AERONAUTICAL RESEARCH COUNCIL

CURRENT PAPERS

The Dynamic Stability Derivatives of a Slender Wing at zero and Moderate Lift A Comparison of Theory with Free-Flight Model Tests, M = 0.8 to 2.0

by

A. Jean Ross, Geraldine F. Edwards and A. P. Waterfall

Aerodynamics Dept., R.A.E., Farnborough

LONDON: HER MAJESTY'S STATIONERY OFFICE

1975

PRICE *85p* NET

533.693.3 : 533.695.16 : 533.6.013.417 : 533.6.013.601

* CP, No.1310

May 1973

THE DYNAMIC STABILITY DERIVATIVES OF A SLENDER WING AT ZERO AND MODERATE LIFT; A COMPARISON OF THEORY WITH FREE-FLIGHT MODEL TESTS, M = 0.8 to 2.0

by

A. Jean Ross
Geraldine F. Edwards
A. P. Waterfall

SUMMARY

The longitudinal and lateral stability derivatives of a slender wing and fin configuration (AGARD 'G' standard model) have been measured at near-zero and at moderate lift using rocket-launched free-flight models. Comparisons are made with theoretical estimates of the derivatives, and with previous experimental results from models flying at near-zero lift. The derivatives showing the greatest dependence on angle of attack are z_w, m_w and ℓ_v. The results also show that the linear theories used for obtaining values of these same derivatives at zero lift are inadequate at transonic speeds.

---

* Replaces RAE Technical Report 73097 - ARC 34897

CONTENTS

1 INTRODUCTION

A series of free-flight model experiments on a simple slender-wing design, known as Orion*, was planned during the early stages of aerodynamic research on such shapes in order to measure stability derivatives at supersonic and transonic speeds.

Most of the results at near-zero lift have already been published[1]; the present report describes additional zero-lift experiments in the transonic region, together with those for models flying at lift. The lifting models had elevators set at -5°, so that the stability derivatives were measured at trimmed angles of attack, dependent on the Mach number, of about 1° at M = 2.0, increasing to about 5° for $M < 1.0$.

The present tests consisted of four lifting model flights (numbered 13, 18, 24 and 25 in the RAE free-flight model 'Orion' series) and three non-lifting models (numbered 19, 20 and 26). Models 19, 20, 24, 25 and 26 were designed to give prolonged flight at transonic speeds (where the derivatives were expected to change rapidly) using the test procedure described in Ref.2.

Results from the present tests are compared with the zero-lift results from Ref.1 and with theoretical estimates. The effect of non-zero angle of attack is shown to be pronounced for the derivatives** z_w, m_w and ℓ_v, but the remaining derivatives $m_q + m_{\dot{w}}$, n_v, ℓ_p and $n_r - n_{\dot{v}}$ are not measurably changed.

A summary report will be published later comparing all the free-flight results, with the values of the derivatives measured using the RAE Bedford wind tunnel oscillatory rig and with theoretical estimates.

2 EXPERIMENTAL TECHNIQUES

The construction and instrumentation of the Orion models is fully described in Ref.1. The geometric details are shown in Fig.1, and listed, with other data, in Table 2. Each model is launched, mounted pick-a-back, on a boost rocket, from which it separates at about M = 2, to perform a near-ballistic

---

* Later adopted as the AGARD 'G' standard wing shape.

** The notation used for the stability derivatives is that of Ref.1, for continuity; the relation to the new notation of Ref.3 is given in Table 1.

trajectory, decelerating to transonic speeds before reaching sea level. Typically, a model would be disturbed from its trimmed flight condition by small pulse rockets, fired at about six preset times during the flight, to give either longitudinal or lateral impulses. The resulting responses were measured by one longitudinal, three normal and three lateral linear accelerometers, and by one roll angular accelerometer. The readings of these transducers were telemetered sequentially to a recording station on the ground. The lifting models also carried an incidence probe in the nose, to give angle of attack.

In order to attain non-zero lift conditions, four of the models were made with inboard half-span elevators of 0.05 c_0 chord, which were fixed at a chosen setting of -5°, as shown in Fig.2. A small differential angle of 1° was also applied to give a steady rolling moment so that these models would execute a barrel-roll about a near-ballistic trajectory[4]. The trimmed lift achieved by these four models is shown in Fig.3.

The non-lifting models Orions 19, 20 and 26 were flown specifically to investigate the variation of the derivatives close to M = 1, using the technique described in Ref.2, although some derivatives could also be obtained at M = 2 from the oscillations occurring when the model separated from the boost rocket. The disturbances applied to the lifting Orions 24 and 25 were also mainly concentrated in the transonic region M = 0.86 to 1.15.

The Reynolds number for the tests was similar to those for the non-lifting models of Ref.1; at M = 2.0, the Reynolds number was about 5×10^7, based on $\bar{c}$, and fell to about 2×10^7 at M = 0.8.

3 ANALYSIS OF DATA

3.1 Trajectory analysis

The space coordinates and velocity of free-flight models at RAE are obtained by the usual weapons-range techniques, e.g. kinetheodolites, radar and radio-Doppler trackings. The test conditions of atmospheric static pressure, temperature, wind speed and direction at the flight altitudes are obtained from radiosonde measurements made at the range, in the present case Aberporth.

A computer programme[5] combines the above trajectory information with the output from model-borne instrumentation to give in-flight angles-of-attack, drag and lift coefficients together with Mach number and dynamic pressure.

3.2 Response analysis

The longitudinal and lateral oscillatory responses of all the zero-lift models of Ref.1 were analysed using a graphical time-vector technique described in Ref.4. The limitations of this technique are that only those parts of the responses judged to be uncoupled motions could be analysed and linear aerodynamics had to be assumed.

For the later models a digital analysis technique[5] was used. This technique utilises a series of computer programmes to mechanise the analysis of the responses, taking due account of non-linear coupling effects.

This technique is an automatic curve-fitting method, based on a variant of the least-squares process, in which estimated initial values of the aerodynamic derivatives are improved iteratively by the computer programmes to values giving a best fit to the measured response data.

The equations of motion constituting the basic mathematical model assumed for the responses are given in the Appendix, and the analysis technique is fully described in Ref.5.

3.3 Presentation of derivatives dependent on angle of attack

Although the lifting Orion models (with elevators set at -5°) were nominally of identical shape, they did not trim at identical angles of attack for a given Mach number, as shown in Fig.3. Thus, in the case of those derivatives which showed significant changes due to angle of attack (z_w, m_w and ℓ_v) the measurements made on the various models could not be compared without first correcting the experimental values to a common mean angle of attack. These corrections were made using the theoretical values of the second-order derivatives, z_{ww}, m_{ww} and ℓ_{vw} as given in section 4.1, i.e.

$$z_w = z_{w_{exp}} - 4(\alpha_{mean} - \alpha_T) \quad (1)$$

$$m_w = m_{w_{exp}} - 1.6(\alpha_{mean} - \alpha_T) \quad (2)$$

$$\ell_v = \ell_{v_{exp}} + \ell_{vw}(\alpha_{mean} - \alpha_T) \quad (3)$$

where α_{mean} and α_T are in radians.

The small contribution expected to the damping-in-pitch derivative, ($0.17\alpha_T$, see section 4.1) gives corrections well within the scatter of the experimental results.

4 THEORETICAL ESTIMATES OF STABILITY DERIVATIVES

4.1 Longitudinal derivatives

The methods of estimation described in Ref.1 are used, but with some modifications for z_w and m_w. The lift and pitching moment both vary non-linearly with angle of attack, and it is assumed that

$$C_L = a_1\alpha + a_2\alpha|\alpha| \tag{4}$$

$$-C_m = m_1\alpha + m_2\alpha|\alpha| \tag{5}$$

so that

$$z_w = -\frac{1}{2}\frac{dC_L}{d\alpha} = -\frac{a_1}{2} - a_2|\alpha| \tag{6}$$

$$m_w = \frac{1}{2}\frac{dC_m}{d\alpha} = -\frac{m_1}{2} - m_2|\alpha| \quad . \tag{7}$$

It has been suggested[6] that a good approximation for the non-linear lift contribution is $a_2 = 4$, for wings of aspect ratio about 1.0, and so equation (6) becomes

$$z_w = z_{w_0} - 4|\alpha| \tag{8}$$

where z_{w_0} is the linear theoretical value given in Ref.1.

The non-linear pitching moment has been calculated by Smith, in some unpublished work, for a mild gothic planform, and he quotes[6] a shift in aerodynamic centre of 0.04 c_0 between $C_L = 0$ and 0.1. Using values of a_1 and m_1 from slender body theory, equations (7) and (8) may be solved, with

$$h - h_0 = -\frac{dC_m}{dC_L} = \frac{m_w}{z_w} \quad ,$$

to give

$$m_2 = 1.6 \quad ,$$

so that

$$m_w = m_{w_0} - 1.6|\alpha| \quad . \tag{9}$$

In Ref.1, three estimates of z_{w_0} and m_{w_0} were shown at supersonic speeds, but only one is given in the present comparison for clarity.

The contribution to damping-in-pitch derivative, due to angle of attack was estimated using the results of Ref.7. Garner and Lehrian considered only a wing of gothic planform, but for the relatively small angles of attack covered in the experiments, it seems sufficient to use their numerical values for $\frac{d}{d\alpha}(m_q + m_{\dot{w}})$ at the appropriate CG position,

$$m_q + m_{\dot{w}} = (m_q + m_{\dot{w}})_{\alpha=0} - 0.17|\alpha| \qquad (10)$$

4.2 Lateral derivatives

Rolling moment due to sideslip, ℓ_v, is the only measured lateral derivative for which reliable estimates of effects due to angle of attack may be made, and so y_v, n_v, ℓ_p and $n_r - n_{\dot{v}}$ are assumed to be independent of α. The methods described in Ref.1 are used for these derivatives, and for estimating $\frac{d\ell_v}{d\alpha}$ $(= \ell_{vw})$.

Estimates of ℓ_r and n_p were required in the analysis of the experimental records, and slender body theory[8] was used to give $\frac{d\ell_r}{d\alpha}$ and $\frac{dn_p}{d\alpha}$. The resulting values of ℓ_r and n_p for the different models are shown in Fig.4.

5 EXPERIMENTAL AND THEORETICAL RESULTS

5.1 Trimmed conditions of lifting models

The trimmed values of normal acceleration, a_z, lift coefficient, C_{L_T}, and angle of attack, α_T, are shown varying with Mach number in Fig.3. Angle of attack for Orion 24 is not presented because of unexplained anomalies in the measurements, but it should not differ significantly from that of the other models. The values assumed in the analysis of Orion 24 results are given in Table 3.

As the lifting models decelerated the trimmed angle of attack increased from about 1° at M = 2.0 to between 2° and 3° at M = 1.1, it then increased rapidly through M = 1.0 to about 5° at subsonic Mach numbers.

5.2 Stability derivatives dependent on angle of attack

The experimental results for the derivatives z_w, m_w and ℓ_v, which varied significantly with angle of attack, are shown in Figs.5 and 6 for zero

and non-zero angle of attack respectively. Fig.5 shows the results from Ref.1, and includes additional results for the models designed to have prolonged flight at transonic speeds[2].

The results for the damping-in-pitch derivative, $m_q + m_{\dot{w}}$, is theoretically dependent on angle of attack, are shown in Fig.8. The values obtained from the lifting models have been adjusted by the small increment $0.17|\alpha_T|$ to give the value of the derivative at $\alpha_T = 0^o$; such increments are within the experimental scatter of the zero-lift results.

5.2.1 z_{w_0}, m_{w_0} and ℓ_{v_0}

There is appreciable scatter in the results for z_{w_0}, and the values obtained from the digital analysis indicate large likely* errors (denoted by the vertical bars on the symbols in Fig.5). The mean curve drawn through the experimental results must therefore be regarded as tentative. The additional results tend to confirm that the theoretical estimates[9,10] of z_{w_0} at transonic speeds are too small in magnitude.

The sudden change in level of m_{w_0} near M = 1.0, indicated in Ref.1, is now defined fairly clearly, and it is possible to choose a mean curve through the experimental results with all but two of the points lying within a scatter-band of ±0.01. It should be noted that the results at subsonic speeds taken from Ref.1 have now been corrected for the small non-zero angle of attack at which the particular model trimmed ($\alpha_T \approx -0.02$ rad), using equations (1) and (2). These subsonic values now give excellent agreement with theory[10]. However, the experimental values depart markedly from theory for $M > 0.96$, with a difference in m_{w_0} of 0.05 at M = 1.0. The maximum magnitude in m_{w_0} occurs at $M \approx 1.3$ experimentally, compared with $M \approx 1.9$ theoretically[11].

The variation of ℓ_{v_0} with supersonic Mach number is remarkably well defined, considering the small absolute value of the derivative, but there is insufficient data to give a subsonic mean value. The additional results do show, however, that the slender-body theory[8] underestimates the magnitude slightly at M = 1.0, giving $\ell_{v_0} = 0.009$ compared with an experimental mean value of 0.02. As noted in Ref.1, the almost constant difference of 0.008

---

* The response analysis programme gives the probable error in each evaluated derivative at the 95% probability level, assuming that the derivatives are uncorrelated with respect to the response. This is not exactly satisfied, and so the actual error may be larger than that shown. The likely errors do, however, indicate the relative accuracies of the evaluated derivatives.

between experiment and theory[12] at supersonic speeds, $M > 1.4$, is small compared with the magnitudes of the direct fin contribution and the wing-fin interference contribution (see Fig.21b of Ref.1) so that the values lie within the expected accuracy of estimation.

5.2.2 z_w, m_w and ℓ_v at lift

As described in section 3.3, the values of the derivatives at non-zero lift (Fig.6) have been corrected to refer to the mean angle of attack, also shown in Fig.6. The actual experimental values are given in Table 3, together with the incremental corrections used, and it may be seen that the maximum corrections are 0.03 for z_w, 0.013 for m_w and 0.008 for ℓ_v. Mean curves have been drawn through the experimental results, and if likely errors are taken into consideration, the scatterbands are ±0.04 for z_w, ±0.01 for m_w (except for one point) and ±0.005 for ℓ_v.

A direct comparison of these experimental results with theory would include the discrepancies already noted in the measurements at zero lift. To provide a comparison for the effects of angle of attack alone, an attempt has been made to obtain experimental values for the second-order derivatives, z_{ww}, m_{ww} and ℓ_{vw}, using the mean curves to give

$$z_{ww} = (z_w - z_{w_0})/\alpha \quad , \quad \text{etc.}$$

Of course, the scatter affects the accuracy, and so it is only possible to indicate trends with Mach number in Fig.7. Also shown are the values of z_{ww} and m_{ww} obtained by analysis of the static tunnel tests for the mild gothic wing 5 of Ref.13, which is geometrically very close to Orion. Very near to $M = 1.0$, the tunnel values tend to give a peak, in both z_{ww} and m_{ww}, with maximum magnitude above the free-flight values, and above the theoretical estimate[6]. The free-flight results for z_{ww} decrease rapidly in magnitude between $M = 1.0$ and 1.1, then remain fairly constant up to $M = 1.4$. No tunnel results are available between $M = 1.02$ and 1.42, but the loss in z_{ww} with increasing M is apparent, with the general level of the tunnel values being above the free-flight results. For m_{ww}, the free-flight results are close to the tunnel results at $M \approx 0.9$ and at 1.4, but there is a factor of 2 difference at $M = 1.0$, so that the variation through the transonic range appears to be quite different. The theoretical estimates of $z_{ww} = -4$ and

$m_{ww} = -1.6$ are both too large in magnitude at supersonic speeds, the mean experimental value for z_{ww} being -2 for $M > 1.2$, and $-m_{ww}$ decreasing from about 1.2 at M = 1.2 to 0.7 at M = 2.0.

For the rolling moment due to incidence and sideslip, ℓ_{vw}, the response analysis programme gave values* when the longitudinal and lateral responses were both of significant magnitude (so that the cross-coupling effects were discernible), and these values are shown as discrete points on Fig.7. The variation of ℓ_{vw} with M obtained for the two experimental mean values of ℓ_v at $\alpha = 0$ and ℓ_v at $\alpha = \alpha_T$ is also shown as the broken curve. Both sets of experimental results are close to theory[8] at M = 1.0, but the values obtained from the coupled responses tend to be smaller in magnitude than theory[14] and the derived values for $1.1 < M < 1.4$. Near M = 2, however, the results from the coupled responses indicate that ℓ_{vw} is again close to the theoretical value.

5.2.3 Damping-in-pitch derivative, $m_q + m_{\dot{w}}$, Fig.8

The results from the non-lifting models, and the results from the lifting models corrected to $\alpha_T = 0^\circ$, are shown together in Fig.8, the largest correction being 0.015, well within the experimental scatter. At supersonic speeds, the damping-in-pitch derivative is smaller than the theoretical values,[15,16] the additional results confirming the trends shown by results of Ref.1. Although the results near M = 1.0 are fairly scattered, they indicate agreement with the sonic[17] theoretical value of $m_q + m_{\dot{w}} \approx -0.5$, so that the damping-in-pitch derivative is of greatest magnitude in the transonic region, reducing again at subsonic speeds[18].

5.3 Stability derivatives theoretically independent of angle of attack

Sideforce due to sideslip, y_v, Fig.9.

The results for y_v indicate no measurable dependence on angle of attack for the present test conditions. There is good general agreement with theory[6,9,10] for this derivative.

Yawing moment due to sideslip, n_v, Fig.10.

Angle of attack appears to have no significant effect on n_v in the range of α_T covered in the tests. Near M = 1.0, Squire's not-so-slender wing theory[9]

* The mathematical model for rolling moment due to sideslip used in the programme is $\ell_v(\alpha = \alpha_T) + \ell_{vw}[\alpha - \alpha_T]$, which is equivalent to the theoretical value $\ell_v(\alpha = 0) + \ell_{vw}\alpha$.

underestimates the measured values, but at other speeds, i.e. subsonic and $M > 1.2$, theoretical values[6,10] are generally greater than experiment.

Damping-in-roll derivative, ℓ_p, Fig.11.

The scatter in the experimental results for the lateral damping derivatives, ℓ_p and $n_r - n_{\dot{v}}$, is large, as are the likely errors given by the analysis programme. For slender configurations at moderate angle of attack, approximations to the damping of the Dutch-roll oscillation show that it is dependent on both $n_r - n_{\dot{v}}$ and ℓ_p. It can be seen in Figs.11 and 12 that where large likely errors are indicated, they occur in both derivatives, since $n_r - n_{\dot{v}}$ and ℓ_p are extracted from the same response record. This is clearly demonstrated by the results for a lifting model at $M = 1.07$ and $M = 1.42$.

Because of the large scatter in the measurements of ℓ_p it is possible to make only qualitative observations based on the general distribution of results. One such observation is that the general level of results from the lifting models at subsonic and transonic speeds appears to be higher than that for the models at zero lift, and this indicates a possible measured effect of angle of attack. At speeds above $M = 1.4$ the scatter is somewhat less, and the mean experimental levels from both the lifting and non-lifting models tend to become lower than theory[19,20]. They also become progressively lower than the results from the steady rolling tests (at zero lift) of Ref.1, as Mach number increases.

Damping-in-yaw derivative, $n_r - n_{\dot{v}}$, Fig.12.

At supersonic speeds there is no apparent dependence of $n_r - n_{\dot{v}}$ on angle of attack, and the additional results indicate a greater reduction in damping as M increases than theory[15,16] predicts. The zero-lift models show that damping is increased near $M = 1.0$, where sonic theory[8] gives $n_r - n_{\dot{v}} \approx -0.4$, instead of -0.3 obtained by interpolation of subsonic and supersonic theories. The majority of the results from the lifting models at subsonic speeds imply that the damping is greater than values given by subsonic theory[18], for the fin contribution.

6 CONCLUSIONS

The longitudinal and lateral stability derivatives of a slender-wing and fin configuration have been measured at zero and at moderate lift using the Orion free-flight models.

Results have been obtained for the derivatives z_w, m_w, $m_q + m_{\dot{w}}$, y_v, n_v, ℓ_v, ℓ_{vw}, ℓ_p, $n_r - n_{\dot{v}}$ over the range of Mach number 0.97 to 2.0 at zero angle of attack, and at angles of attack ranging from about 5^o at M = 0.8 to about 1^o at M = 2.0. These results have been compared with the more extensive zero angle of attack results from Ref.1 for the same Orion wing/fin configuration, and the following conclusions have been reached. The change in m_w transonically, at zero lift, is much more abrupt than not-so-slender wing theory predicts, and the derivative z_w is larger in magnitude near M = 1 than the value given by slender body theory. The derivatives z_w and m_w also appear to depend strongly on angle of attack at lower Mach numbers, but it is difficult to assess how well non-linear theory accounts for this variation because of the inadequacy of the basic linear theory in the transonic region. The results for damping-in-pitch derivative show no measurable dependence on angles of attack of the present magnitude.

The lateral derivatives generally behave as theory predicts as Mach number and angle of attack vary although n_v and ℓ_v, at zero lift, are more dependent on M in the transonic region. As expected, ℓ_v was the only lateral derivative to show significant variations with angle of attack.

For most of the derivatives, the values estimated using existing linear theories are in reasonable agreement with the experimental results for the ranges of angle of attack likely to be of interest, but z_w, m_w and ℓ_v, which are expected to be highly dependent on the angle of attack, appear to need more accurate theories at transonic speeds than those used in this comparison.

Acknowledgment

The experiments on Orions 1 to 18 were designed and carried out by K.J. Turner and G.K. Hunt, and the data for this Report were collated by G.H. Greenwood.

Appendix

EQUATIONS OF MOTION USED IN DIGITAL ANALYSIS

The equations of motion used as the basis of the least-squares fitting technique are listed below, together with the relationships between the accelerations measured with respect to moving and earth-fixed axes.

$$\dot{w} = z_w w\rho SV/m + qV - pv + g \cos\theta \cos\phi$$

$$\dot{q} = m_w w\rho S\bar{V}\bar{c}/I_y + (m_q + m_{\dot{w}})q\rho S\bar{V}\bar{c}^2/I_y + m_t\rho SV^2 s/I_y + b_y pr$$

$$\dot{v} = y_v v\rho SV/m + pw - rV + g \cos\theta \sin\phi$$

$$\dot{p} = \ell_v v\rho SVs/I_x + \ell_p p\rho SVs^2/I_x + \ell_r r\rho SVs^2/I_x + \ell_{vw} vw\rho Ss/I_x + \ell_t \rho V^2 Ss/I_x + b_x qr$$

$$\dot{r} = n_v v\rho SVs/I_z + n_p p\rho SVs^2/I_z + (n_r - n_{\dot{v}})\rho SVs^2/I_x + n_{vw} vw\rho Ss/I_z + n_t \rho V^2 Ss/I_z + b_z pq$$

$$\dot{V} = -\rho SV^2 C_D/2m - g \sin\theta$$

$$\dot{\theta} = -g \cos\theta/V$$

$$\dot{\phi} = p$$

$$\dot{z} = V \sin\theta$$

$$a_y = y_v v\rho SV/m + (pq + \dot{r})x_1 - (p^2 + r^2)y_1 + (qr - \dot{p})z_1$$

$$a_z = z_w w\rho SV/m + (pr - \dot{q})x_1 + (qr + \dot{p})y_1 - (p^2 + q^2)z_1$$

For the models with an incidence probe in the nose, the pressure readings are related to the local angles of attack and sideslip,

$$C_{p_w} = \rho VK_w(w - qx_p)$$

$$C_{p_v} = \rho VK_v(v - rx_p)$$

where K_w and K_v are obtained from the calibration of the probe, and x_p is the distance of the probe from the CG. The probe data may also be used in the least-squares fitting process.

As for the graphical analysis, the derivatives ℓ_r and n_p are assumed to be known, and given by the theoretical estimates. The moment equations also contain terms in ℓ_t, m_t, n_t to represent the moments due to the control settings.

Table 1 - NOTATION FOR STABILITY DERIVATIVES

Present report (and Ref.1)		Ref.3	
Symbol	Definition*	Symbol	Relationship**
ℓ_p	$L_p/\rho VSs^2$	$\breve{L}_p$	$\frac{2s^2}{\ell_2^2}\ell_p$
ℓ_r	$L_r/\rho VSs^2$	$\breve{L}_r$	$\frac{2s^2}{\ell_2^2}\ell_r$
ℓ_v	$L_v/\rho VSs$	$\breve{L}_v$	$\frac{2s}{\ell_2}\ell_v$
m_q	$M_q/\rho VS\bar{c}^2$	$\breve{M}_q$	$\frac{2\bar{c}^2}{\ell_1^2}m_q$
$m_{\dot{w}}$	$M_{\dot{w}}/\rho S\bar{c}^2$	$\breve{M}_{\dot{w}}$	$\frac{2\bar{c}^2}{\ell_1^2}m_{\dot{w}}$
m_w	$M_w/\rho VS\bar{c}$	$\breve{M}_w$	$\frac{2\bar{c}}{\ell_1}m_w$
n_p	$N_p/\rho VSs^2$	$\breve{N}_p$	$\frac{2s^2}{\ell_2^2}n_p$
n_r	$N_r/\rho VSs^2$	$\breve{N}_r$	$\frac{2s^2}{\ell_2^2}n_r$
$n_{\dot{v}}$	$N_{\dot{v}}/\rho Ss^2$	$\breve{N}_{\dot{v}}$	$\frac{2s^2}{\ell_2^2}n_{\dot{v}}$
n_v	$N_v/\rho VSs$	$\breve{N}_v$	$\frac{2s}{\ell_2}n_v$
y_v	$Y_v/\rho VS$	$\breve{Y}_v$	$2y_v$
z_w	$Z_w/\rho VS$	$\breve{Z}_w$	$2z_w$

* Definitions of basic symbols are given in the list of symbols

** ℓ_1 and ℓ_2 are the representative lengths for the longitudinal and lateral stability derivatives, respectively

Table 2

MODEL DATA

Geometry

Wing:	planform area	12.813 ft^2		1.19 m^2
	aspect ratio		0.865	
	planform parameter, P		0.578	
	span/length ratio		0.5	
	geometric mean chord, $\bar{c}$	3.853 ft		1.17 m
	volume	1.926 ft^3		0.0545 m^3
	thickness/chord ratio on centre line		0.065	
	Newby area distribution		4 st x(1 - x)	
	zero camber and twist			
Fin:	area (gross)	1.281 ft^2		0.119 m^2
	aspect ratio		0.695	
	geometric mean chord, $\bar{c}_F$	1.379 ft		0.42 m
Centre of gravity			0.5 c_0	

Typical weights and inertias

(a) Models designed for sustained transonic speeds (Orions 19, 20, 24, 25, 26)

Weight		304 lb	138 kg
inertia in roll,	I_x	2.0 slugs ft^2	2.7 kg m^2
inertia in pitch,	I_y	20.6 slugs ft^2	28.0 kg m^2
inertia in yaw,	I_z	21.6 slugs ft^2	29.3 kg m^2
product of inertia,	$I_{xz} \simeq 0$		

(b) Remaining models

Weight		250 lb	113.4 kg
inertia in roll,	I_x	1.6 slugs ft^2	2.17 kg m^2
inertia in pitch,	I_y	19.8 slugs ft^2	26.8 kg m^2
inertia in yaw,	I_z	20.3 slugs ft^2	27.5 kg m^2
product of inertia,	$I_{xz} \approx 0$		

Table 3

EXPERIMENTAL RESULTS FOR LIFTING ORIONS

M	Experimental values				Corrections to mean value				Orion model No.
	α_T	$-z_w$	$-m_w$	$-\ell_v$	$\Delta\alpha$	$-\Delta z_w$	$-\Delta m_w$	$-\Delta\ell_v$	
1.95	0.015	0.57	0.156	0.021	-0.005	-0.02	-0.008	-0.005	25
1.89	0.010	0.63	0.170	0.019	0				13
1.80	0.010			0.021	0				13
1.645	0.011	0.66	0.178	0.019	0.002	0.01	0.003	0.002	13
1.42	0.018	0.78	0.188	0.022	0.002	0.01	0.003	0.002	24
1.29	0.030	0.78	0.218	0.025	-0.003	-0.01	-0.005	-0.003	18
1.14	0.038	0.81	0.211	0.023	0				25
1.09	0.050	0.84	0.214	0.027	-0.008	-0.03	-0.013	-0.008	18
1.07	0.050	0.96	0.207	0.028	-0.006	-0.02	-0.010	-0.006	24
1.00	0.050	0.91	0.217	0.034	0				24
0.965	0.082	0.90	0.203	0.063	-0.002	-0.01	-0.003	-0.002	24
0.93	0.082			0.065	0				24
0.925	0.080	0.93	0.169	0.064	0.002	0.01	0.003	0.002	24
0.92	0.084	1.00	0.203		-0.002	-0.01	-0.003		24
0.91	0.080	0.86	0.186	0.063	0.0025	0.01	0.004	0.003	24
0.89	0.080			0.057	0.004			0.004	18
0.88	0.088			0.070	-0.004			-0.004	24
0.86	0.089	0.98	0.195	0.074	-0.004	-0.02	-0.006	-0.004	24
0.82	0.080			0.052	0.006			0.006	18

SYMBOLS

A	aspect ratio
a_1, a_2	coefficients in expansion of C_L, (equation (1))
a_x, a_y, a_z	components of acceleration
b	span
b_x, b_y, b_z	inertia ratios, $b_x = (I_z - I_y)/I_x$, etc
C_D	drag coefficient, $D/\frac{1}{2}\rho V^2 S$
C_L	lift coefficient, $L/\frac{1}{2}\rho V^2 S$
C_m	pitching moment coefficient, $M/\frac{1}{2}\rho V^2 S\bar{c}$
c_0	root chord
$\bar{c}$	geometric mean chord
D	drag
g	acceleration due to gravity
I_x, I_y, I_z	moments of inertia in roll, pitch and yaw, respectively
I_{xz}	product of inertia
L	lift
$\mathcal{L}$	rolling moment
L_p, L_r, L_v	rolling moment derivatives, $L_p = \partial\mathcal{L}/\partial p$ etc
ℓ_p, ℓ_r, ℓ_v	see Table 1
ℓ_t	rolling moment coefficient associated with trim
ℓ_{vw}	$\frac{d\ell_v}{d\alpha}$, per radian
M	Mach number
$\mathcal{M}$	pitching moment
M_q, M_w, $M_{\dot{w}}$	pitching moment derivatives, $M_q = \partial\mathcal{M}/\partial q$ etc
m_q, m_w, $m_{\dot{w}}$	see Table 1
m_{w_0}	value of m_w at $\alpha = 0$
m	mass of model
m_t	pitching moment coefficient associated with trim
m_1, m_2	coefficients in expansion of C_m (equation (2))

SYMBOLS (concluded)

N	yawing moment
N_p, N_r, N_v, $N_{\dot{v}}$	yawing moment derivatives, $N_p = \partial N/\partial p$ etc
n_p, n_r, n_v, $n_{\dot{v}}$	see Table 1
n_t	yawing moment coefficient associated with trim
P	planform parameter, S/bc_0
p, q, r	rates of roll, pitch and yaw respectively
S	wing area
s	wing semispan
$\hat{t}$	unit of aerodynamic time, $m/\rho SV$
V	velocity along flight path
v	lateral perturbation velocity
w	normal perturbation velocity
x, y, z	body-fixed axes with origin at CG, x positive forward
x_1, y_1, z_1	coordinates of position of accelerometer
Y	sideforce
Y_v	sideforce derivative, due to sideslip, $Y_v = \partial Y/\partial v$
y_v	see Table 1
Z	normal force
Z_w	normal force derivative due to normal velocity, $Z_w = \partial Z/\partial w$
z_w	see Table 1
z_{w_0}	value of z_w at $\alpha = 0$
$\bar{z}$	altitude
α	angle of attack, $\approx w/V$
θ	flight path angle to horizontal
ρ	air density
ϕ	bank angle

Suffixes

T	trimmed value
0	value at $\alpha = 0$

REFERENCES

No.	Author	Title, etc.
1	K.J. Turner A. Jean Ross Geraldine Earley	The dynamic stability derivatives of a slender wing, a comparison of theory with free-flight model tests at near-zero lift, M = 0.8 to 2.4 ARC CP 995 (1966)
2	A.P. Waterfall	An improved technique of stability testing in free flight at transonic speeds, applied to a non-lifting slender wing. ARC CP 1174 (1969)
3	H.R. Hopkin	A scheme of notation and nomenclature for aircraft dynamics and associated aerodynamics. ARC R & M 3562, Parts 1 to 5 (1966)
4	K.J. Turner	Measurements of dynamic stability from three simplified free-flight models of a supersonic research aircraft (Bristol T188) over the Mach number range 1.2 to 2.6. ARC CP 816 (1961)
5	A.P. Waterfall	A technique for the automatic digital analysis of flight dynamic response data. ARC R & M 3699 (1970)
6	J.H.B. Smith J.A. Beasley A. Stevens	Calculations of the lift slope and aerodynamic centre of cropped delta wings at supersonic speeds. ARC CP 562 (1960)
7	H.C. Garner D.E. Lehrian	Pitching derivatives for a gothic wing oscillating about a mean incidence ARC CP 695 (1963)
8	A.H. Sacks	Aerodynamic forces, moments and stability derivatives for slender bodies of general cross-section. NACA TN 3283 (1954)
9	L.C. Squire	Some applications of 'not-so-slender' wing theory to wings with curved leading edges. ARC R & M 3278 (1960)

REFERENCES (continued)

No.	Author	Title, etc.
10		Aerodynamics data sheets. Roy. Aero. Soc.
11	A. Roberts	Development of linear supersonic wing design methods. BAC (Operating) Ltd., M.A. Report 9 (1968)
12	F.S. Malvestuto	Theoretical supersonic force and moment coefficients on a sideslipping vertical and horizontal tail combination with subsonic leading edges and supersonic trailing edges. NACA TN 3071 (1954)
13	L.C. Squire	The characteristics of some slender cambered gothic wings at Mach numbers for 0.4 to 2.0. ARC R & M 3370 (1962)
14	H.S. Ribner F.S. Malvestuto	Stability derivatives of triangular wings at supersonic speeds. NACA TN 1572 (1948)
15	F.S. Malvestuto D.M. Hoover	Lift and pitching derivatives of thin sweptback tapered wings with streamwise tips and subsonic leading edges at supersonic speeds. NACA TN 2294 (1951)
16	F.S. Malvestuto D.M. Hoover	Supersonic lift and pitching moment of thin sweptback tapered wings produced by constant vertical acceleration, subsonic leading edges and supersonic trailing edges. NACA TN 2315 (1951)
17	M.I. Landahl	The flow around oscillating low-aspect-ratio wings at transonic speeds. KTH Aero TN 40 (1954)
18	H.C. Garner	Multhopp's subsonic lifting-surface theory of wings in slow pitching oscillations. ARC R & M 2885 (1952)

REFERENCES (concluded)

No.	Author	Title, etc.
19	F.S. Malvestuto K. Margolis H.S. Ribner	Theoretical lift and damping-in-roll at supersonic speeds of thin sweptback tapered wings with streamwise tips, subsonic leading edges and supersonic trailing edges. NACA Report 970 (1950)
20	H.S. Stone	Aileron characteristics and certain stability derivatives for low-aspect-ratio wings at subsonic speeds. Cornell Aero Lab., Report AF-743-A-3 (1952)

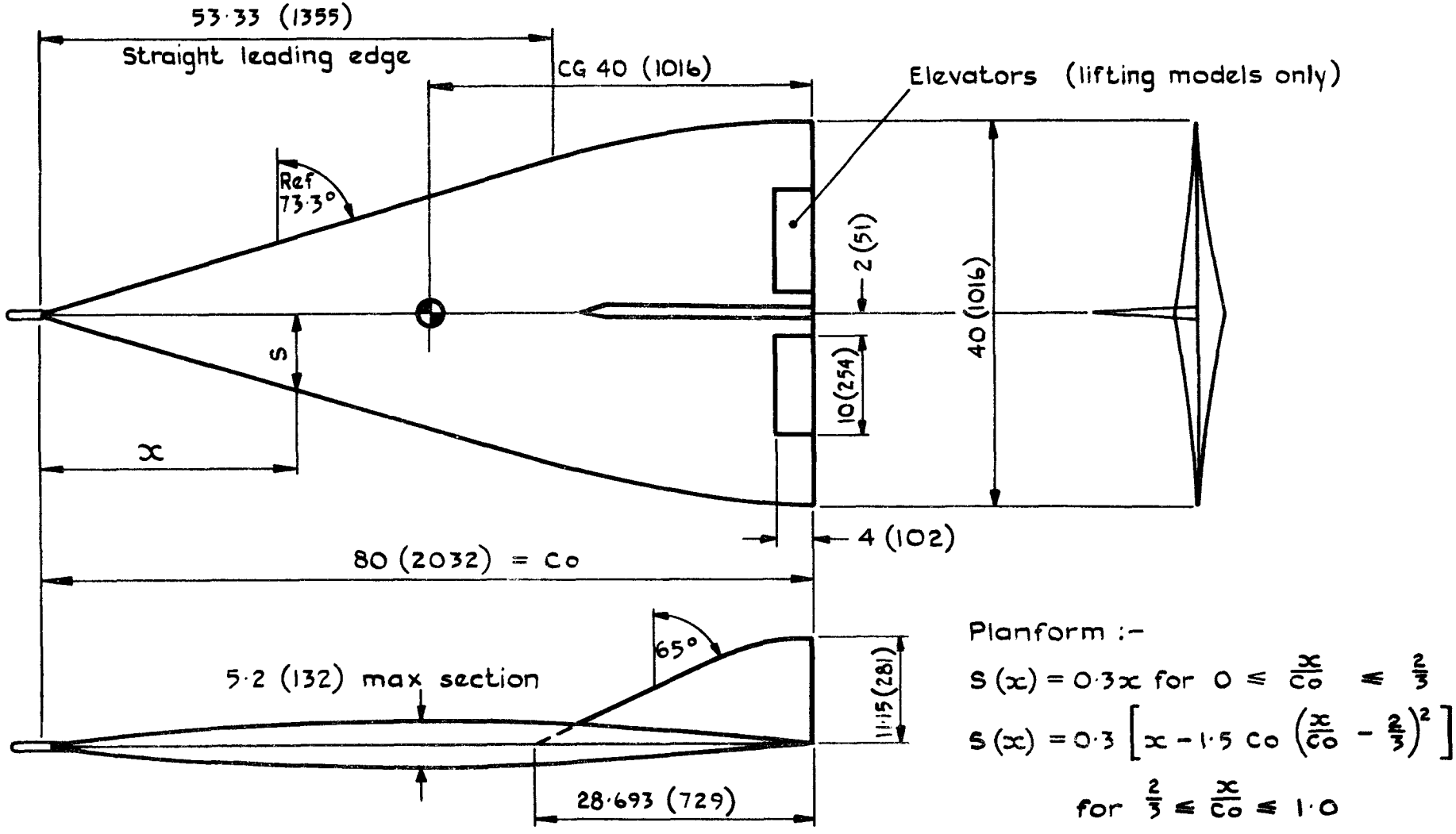

Fig.1 Model geometry

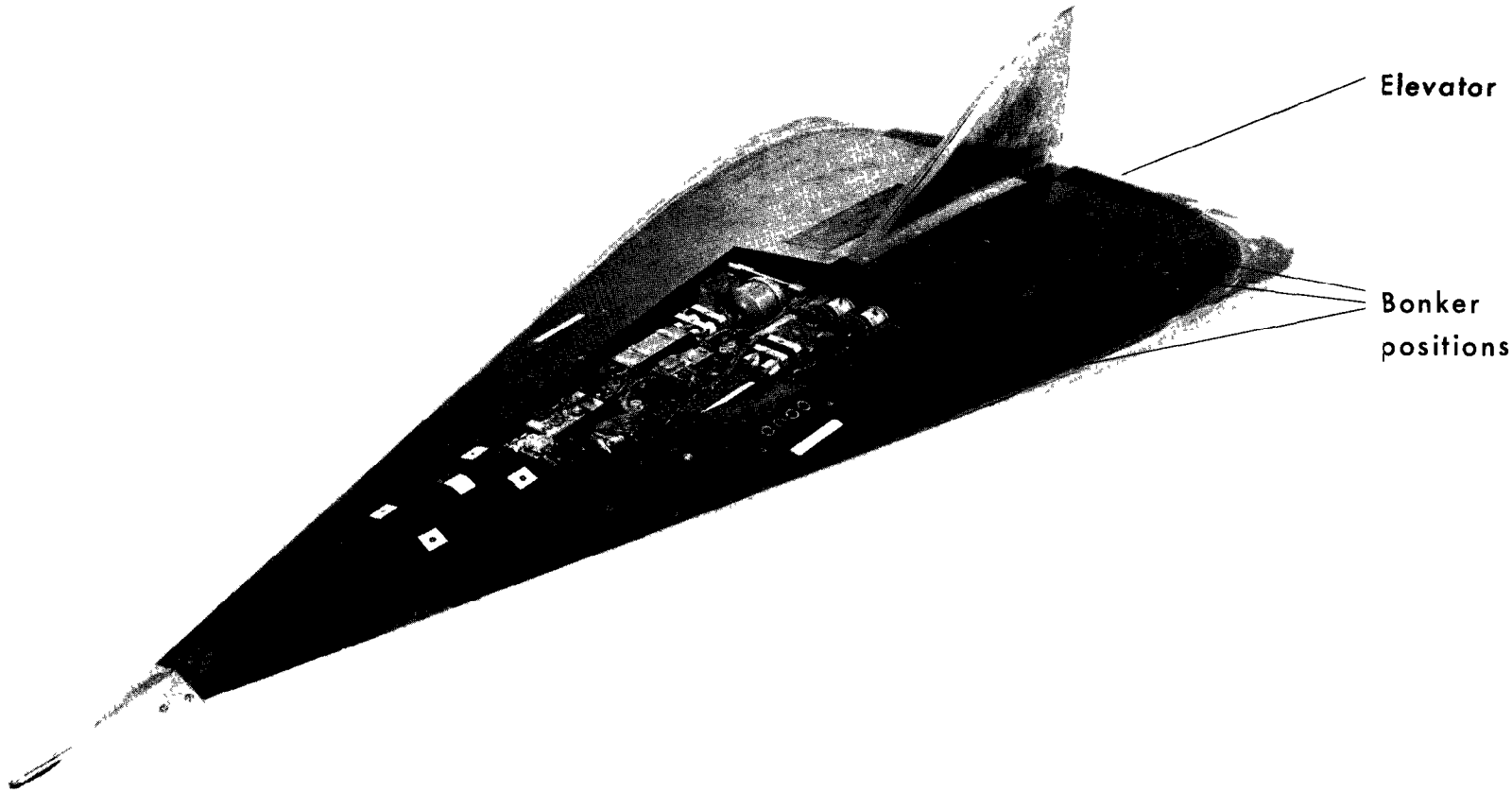

Fig.2. Orion 18, showing instrumentation bay and elevators

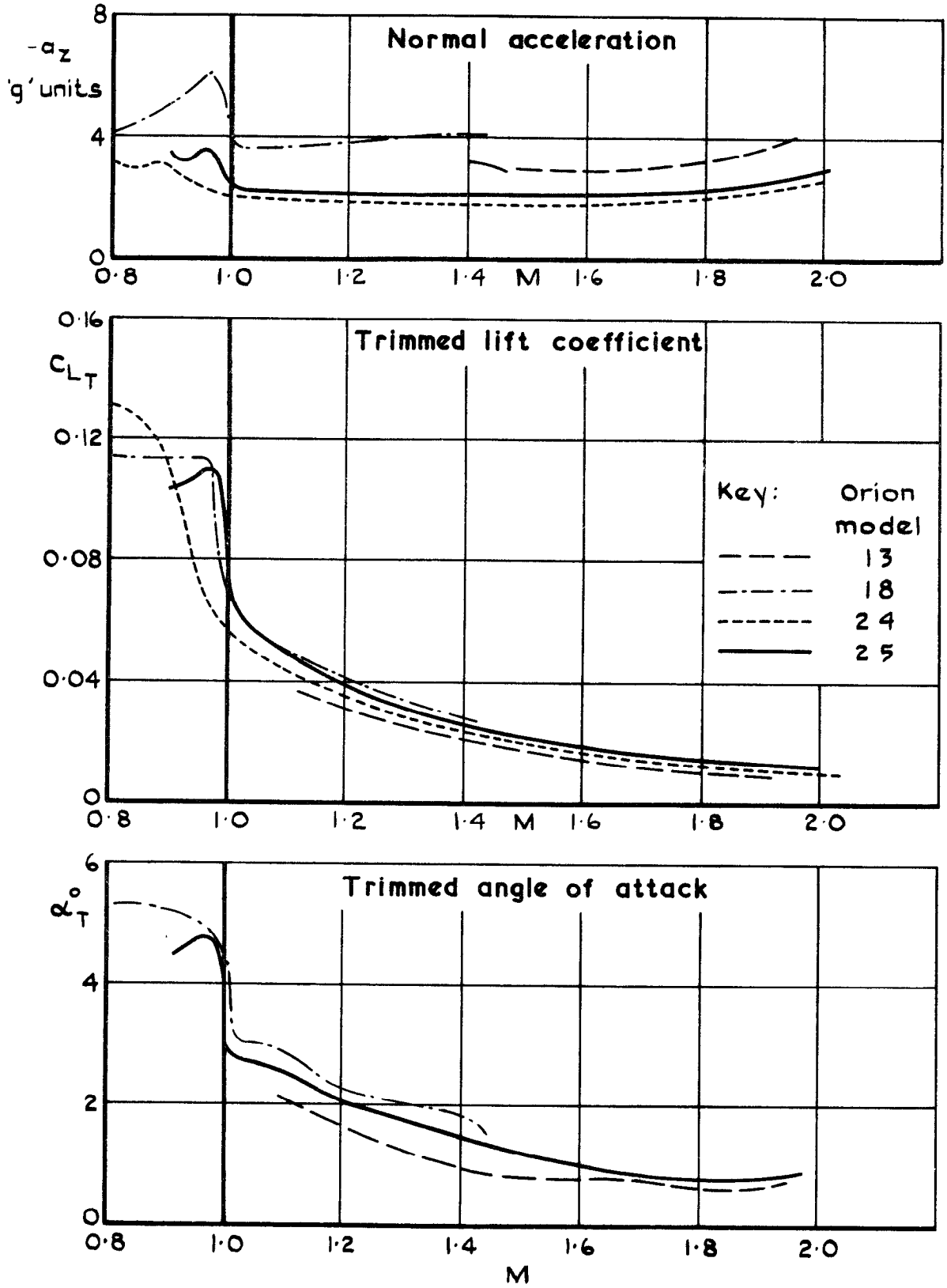

Fig. 3 Trimmed conditions for lifting models

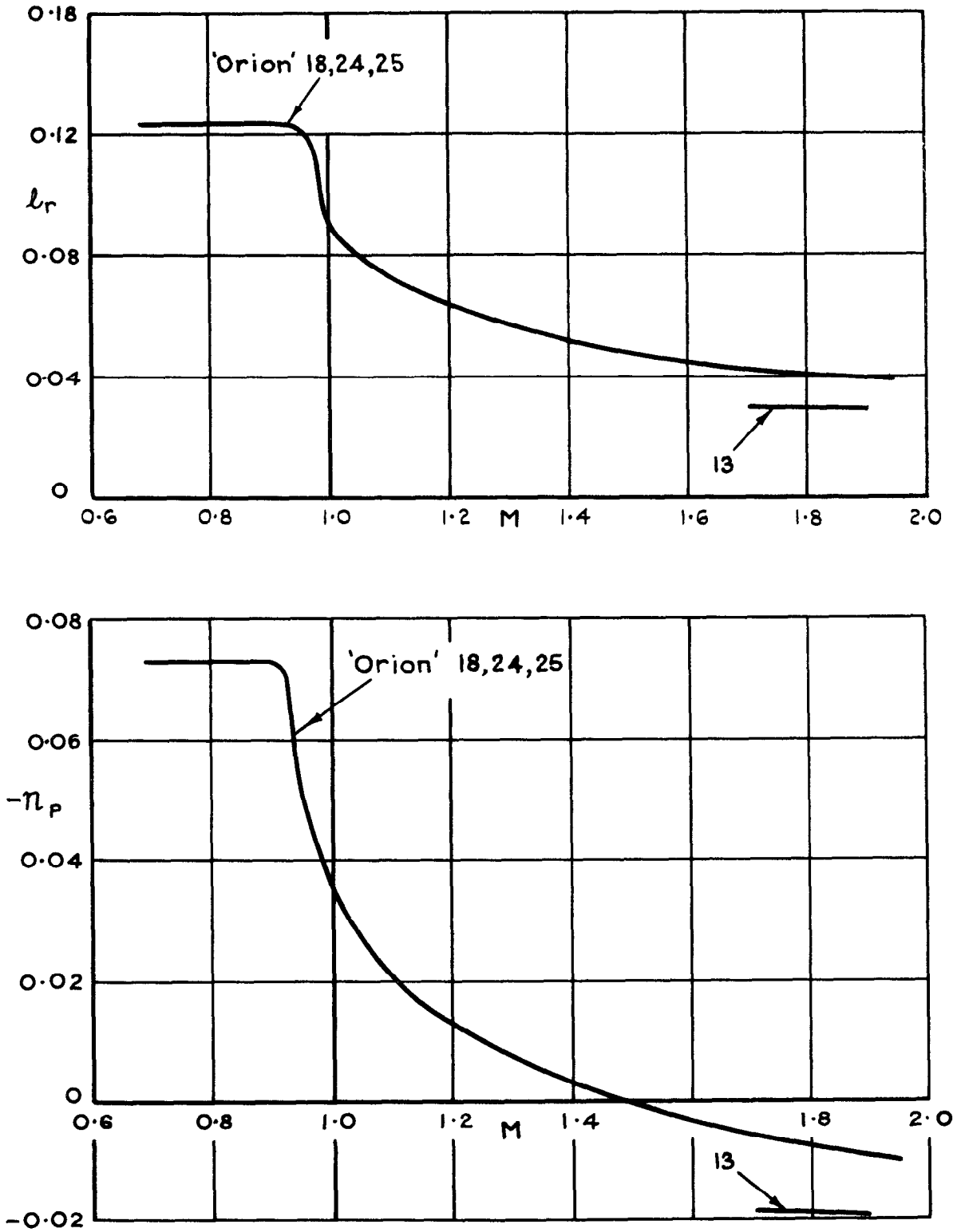

Fig.4 Estimated derivatives l_r and n_p for lifting models

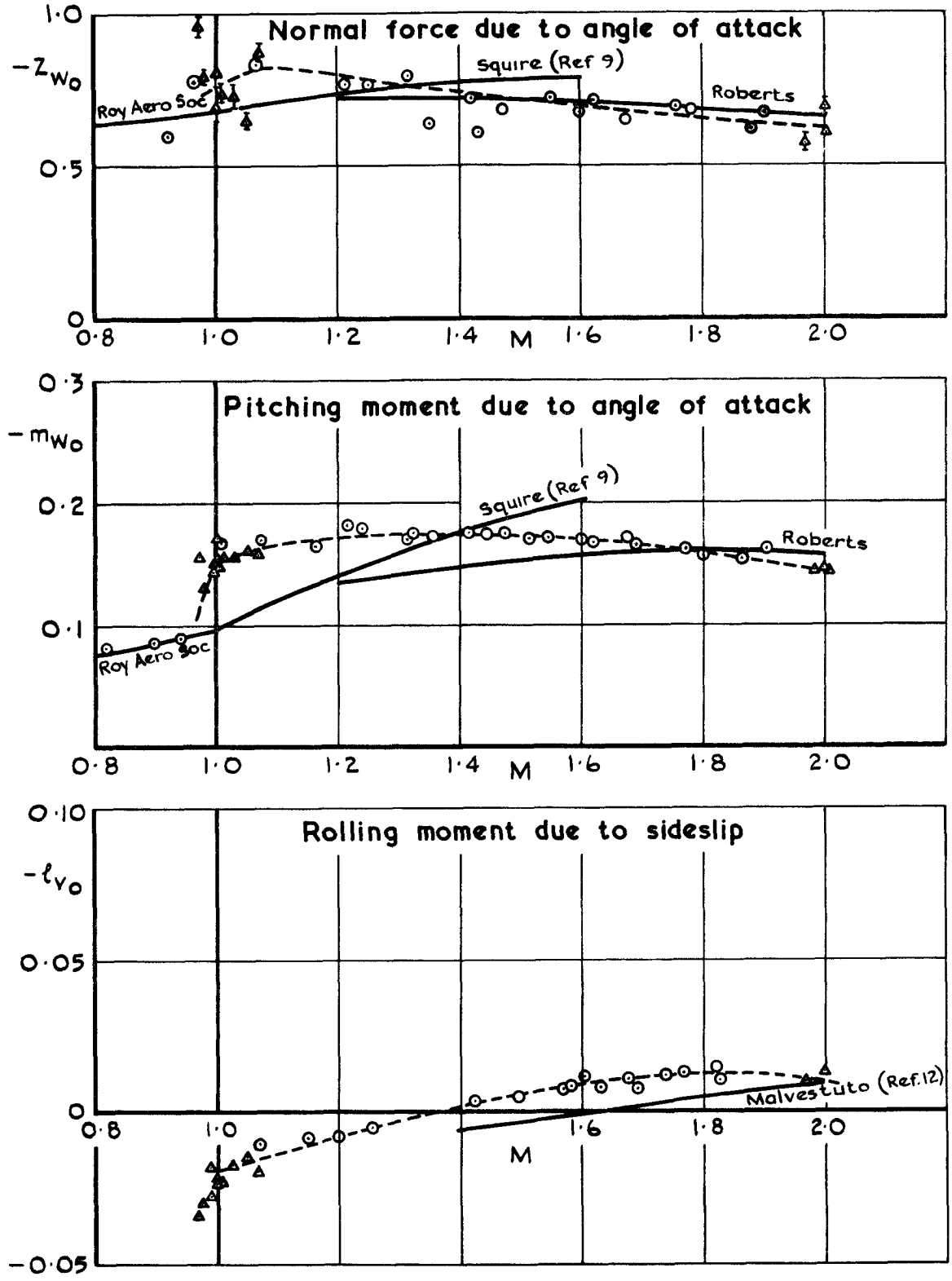

Fig. 5 Derivatives measured at zero angle of attack

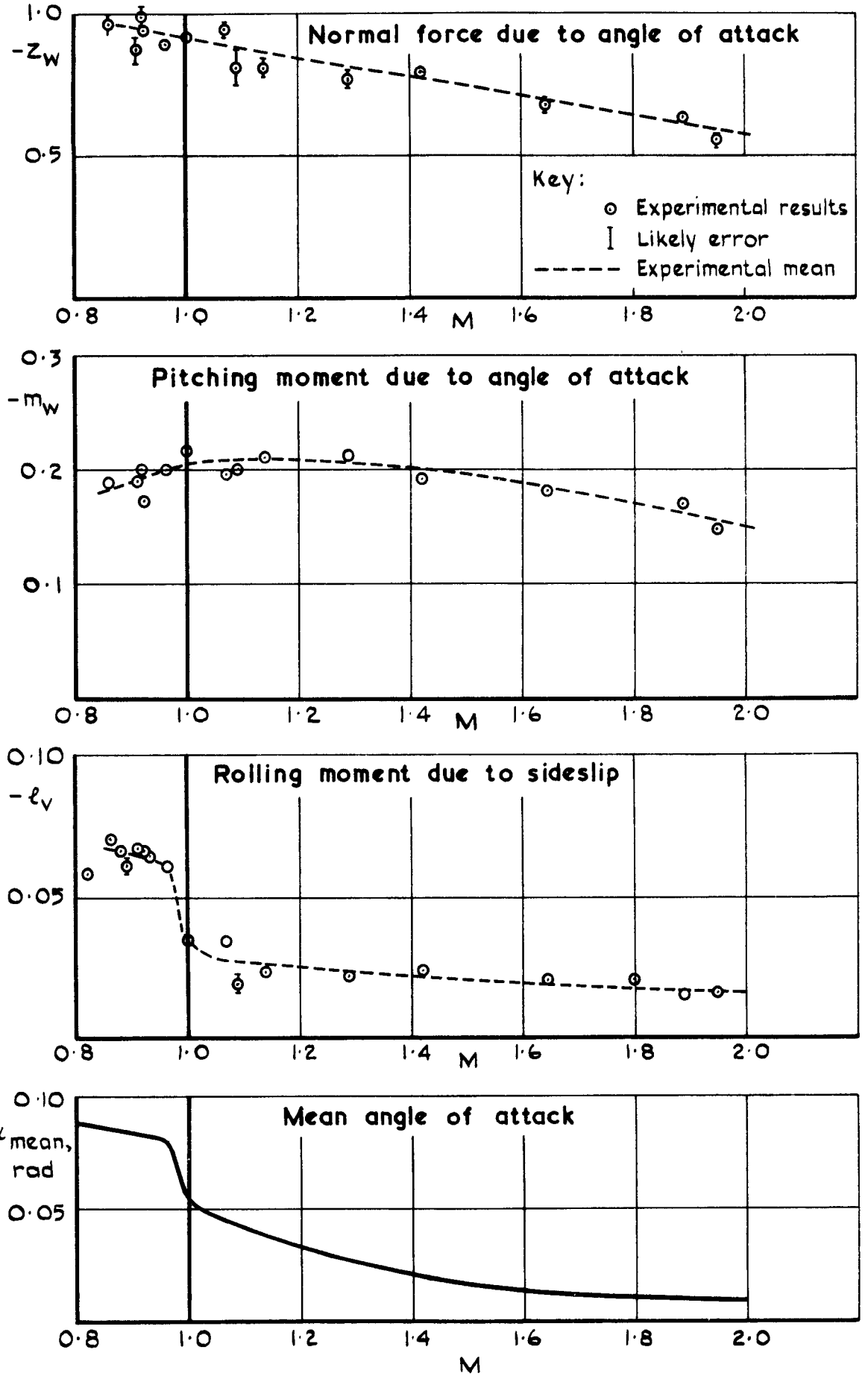

Fig. 6 Derivatives measured at non-zero angle of attack

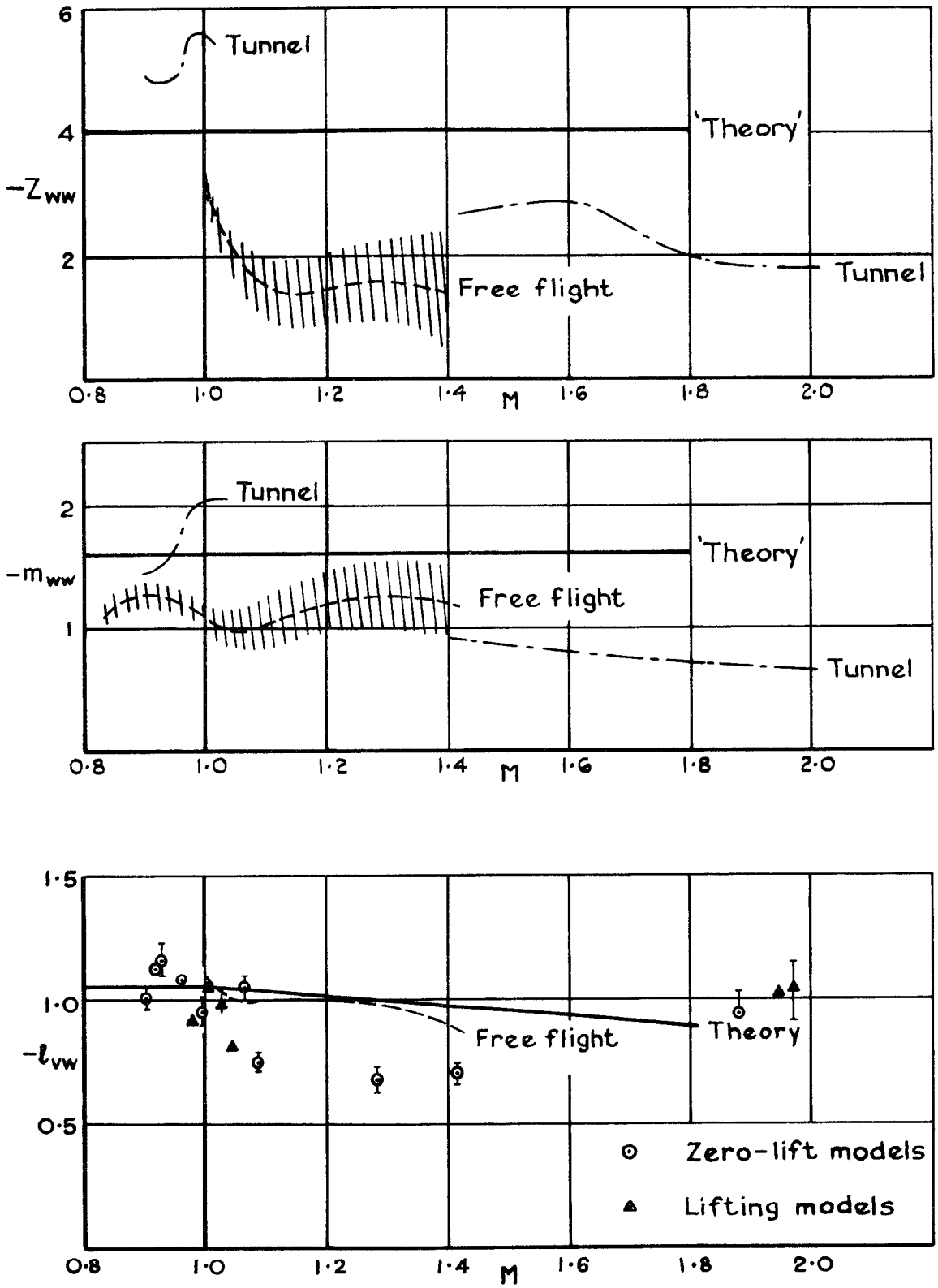

Fig.7 Derived second order derivatives

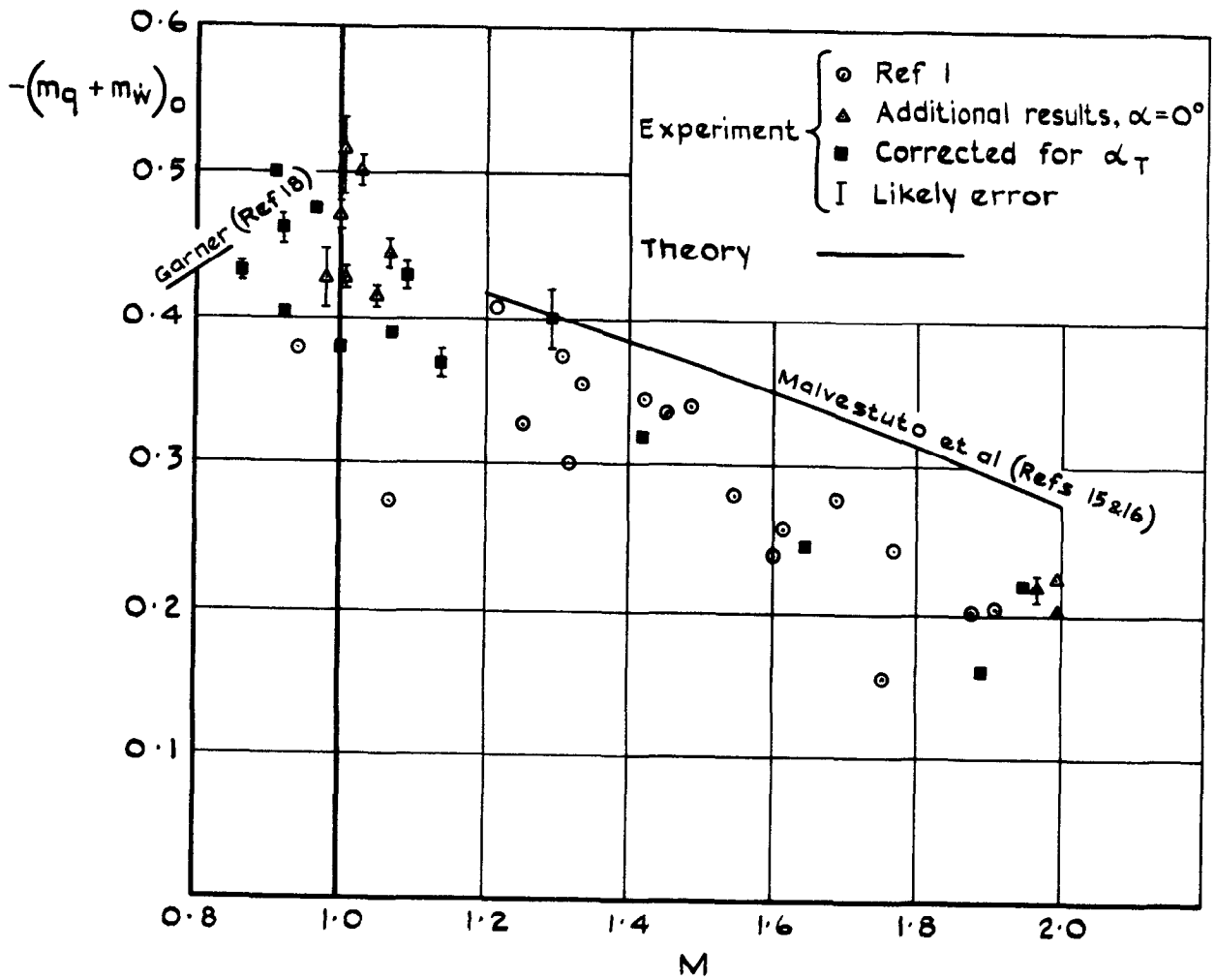

$$\left((m_q + m_{\dot{w}})_o = m_q + m_{\dot{w}} + 0{\cdot}17\,\alpha_T\right)$$

Fig. 8 Damping-in-pitch derivative at $\alpha = 0°$, $\left(m_q + m_{\dot{w}}\right)_o$

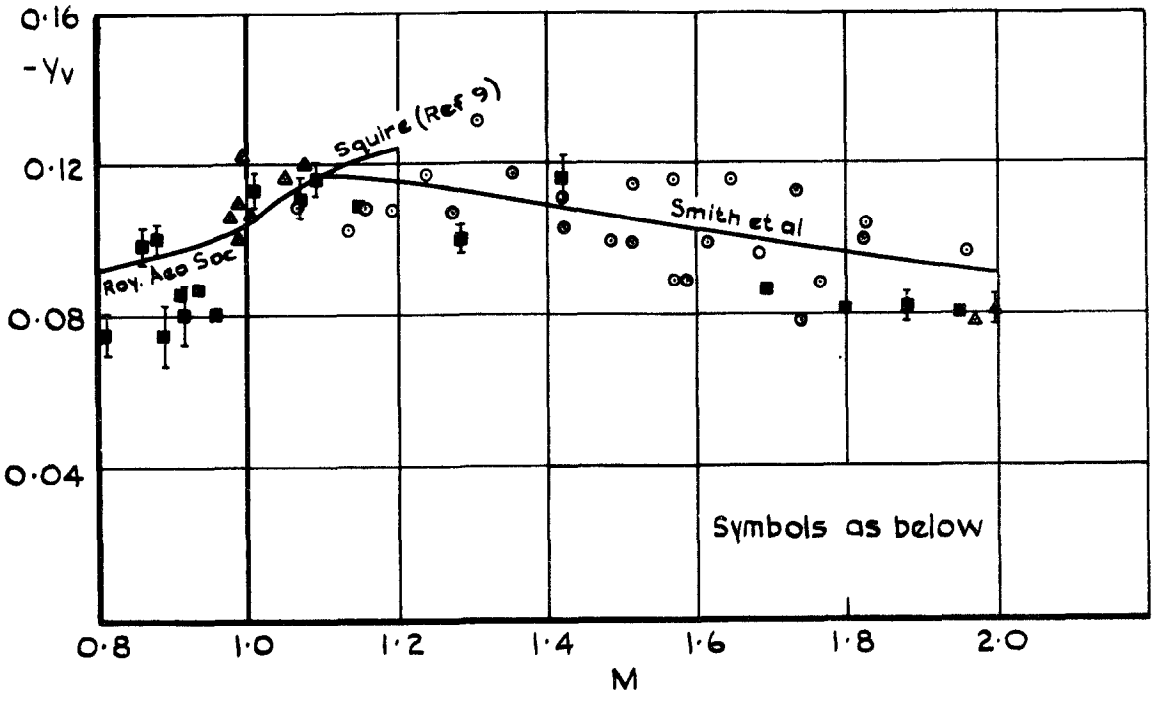

Fig. 9 Sideforce due to sideslip, y_v

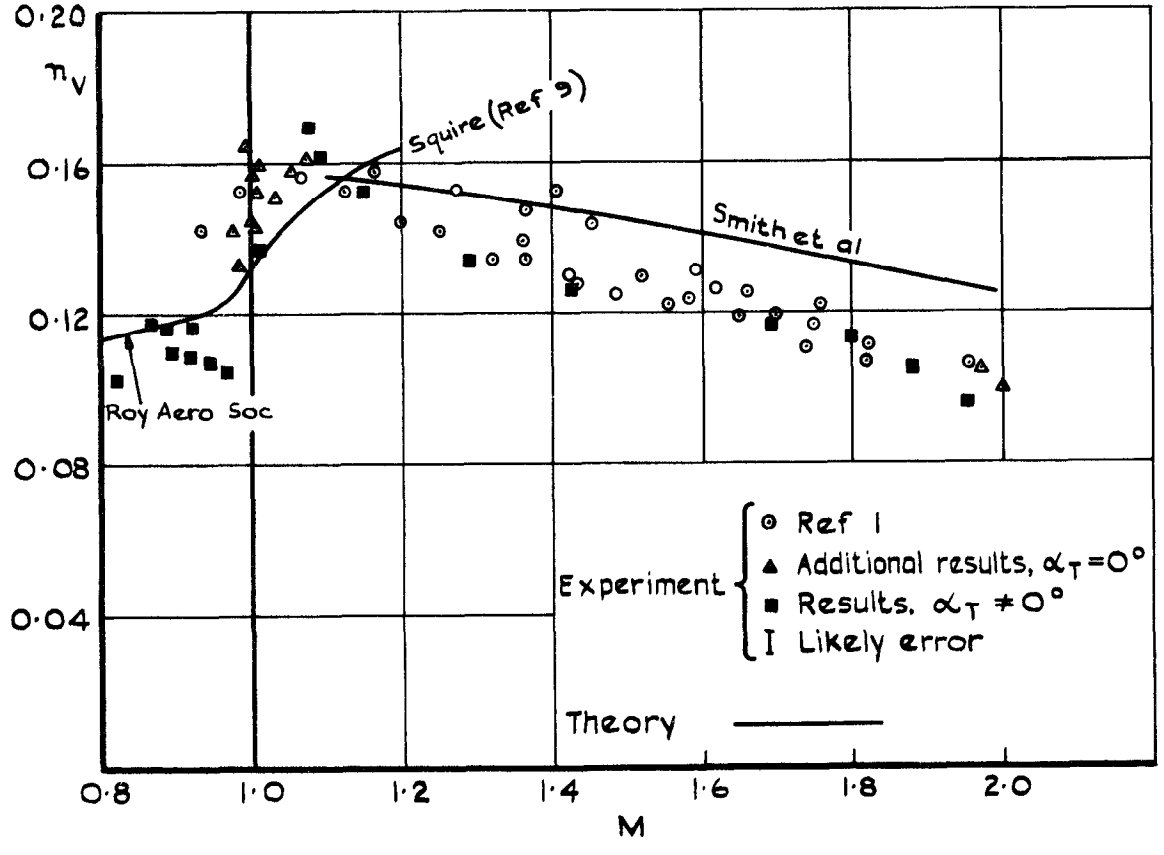

Fig. 10 Yawing moment due to sideslip, n_v

Fig. 9 & 10 Side force and yawing moment due to sideslip

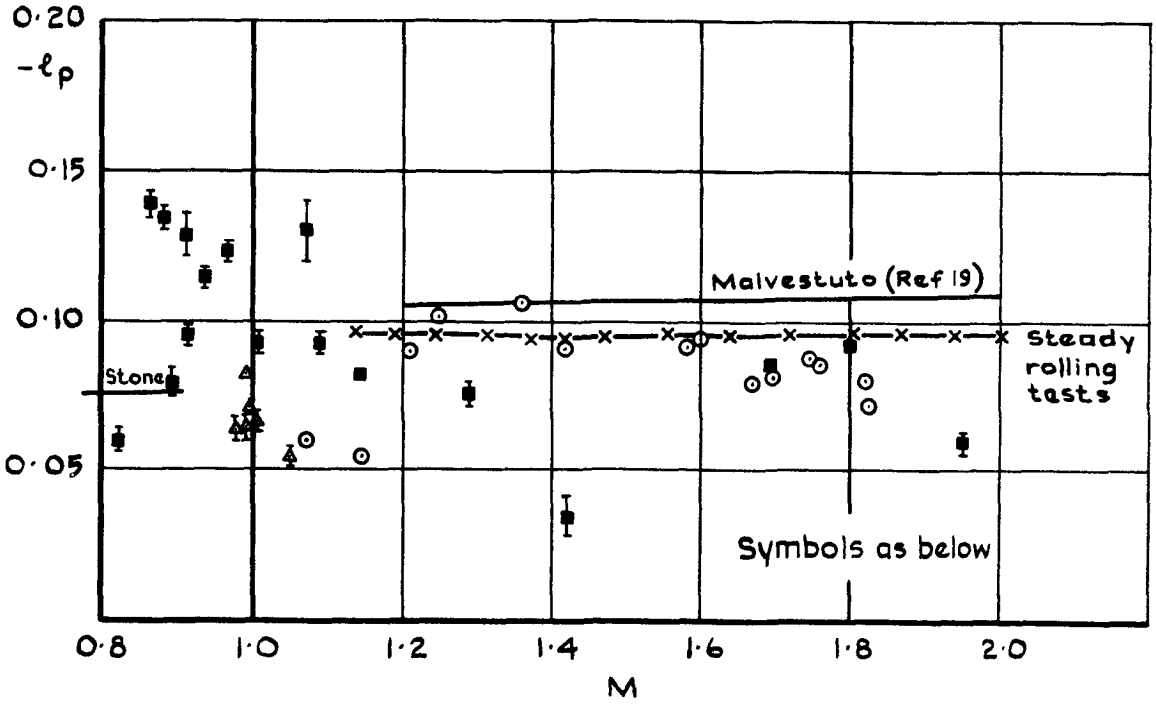

Fig.11 Damping-in-roll derivative, ℓ_p

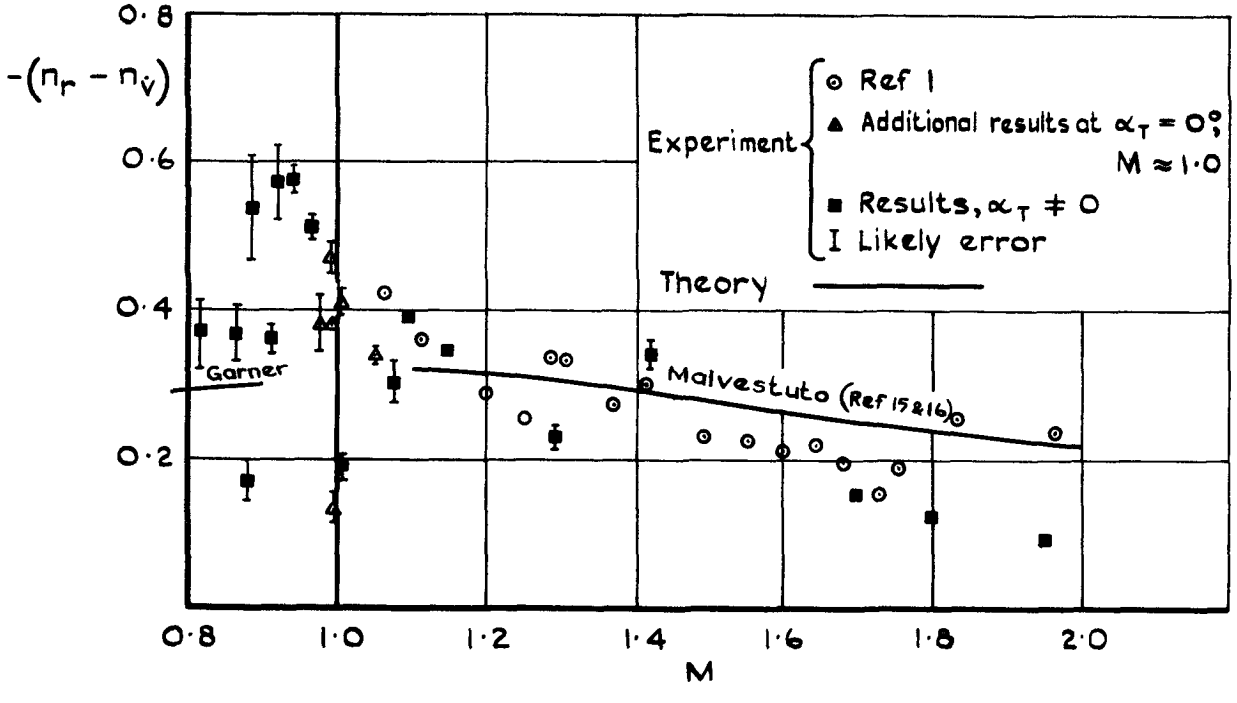

Fig.12 Damping-in-yaw derivative, $n_r - n_{\dot{v}}$

Fig.11 & 12 Damping derivatives in roll and yaw

Printed in England for Her Majesty's Stationery Office by the Royal Aircraft Establishment, Farnborough, Dd 505376 K4 12/74

ARC CP No.1310
May 1973

Ross, A. Jean
Edwards, Geraldine F.
Waterfall, A. P.

533.693.3 :
533.695.16 :
533.6.013.417 ·
533.6.013.601

THE DYNAMIC STABILITY DERIVATIVES OF A SLENDER WING AT ZERO AND MODERATE LIFT, A COMPARISON OF THEORY WITH FREE-FLIGHT MODEL TESTS, M = 0.8 TO 2.0

The longitudinal and lateral stability derivatives of a slender wing and fin configuration (AGARD 'G' standard model) have been measured at near-zero and at moderate lift using rocket-launched free-flight models. Comparisons are made with theoretical estimates of the derivatives, and with previous experimental results from models flying at near-zero lift. The derivatives showing the greatest dependence on angle of attack are z_w, m_w and ℓ_v. The results also show that the linear theories used for obtaining values of these same derivatives at zero lift are inadequate at transonic speeds.

ARC CP No.1310
May 1973

Ross, A. Jean
Edwards, Geraldine F.
Waterfall, A. P.

533.693.3 :
533.695.16 :
533.6.013.417
533.6.013.601

THE DYNAMIC STABILITY DERIVATIVES OF A SLENDER WING AT ZERO AND MODERATE LIFT; A COMPARISON OF THEORY WITH FREE-FLIGHT MODEL TESTS, M = 0.8 TO 2.0

The longitudinal and lateral stability derivatives of a slender wing and fin configuration (AGARD 'G' standard model) have been measured at near-zero and at moderate lift using rocket-launched free-flight models. Comparisons are made with theoretical estimates of the derivatives, and with previous experimental results from models flying at near-zero lift. The derivatives showing the greatest dependence on angle of attack are z_w, m_w and ℓ_v. The results also show that the linear theories used for obtaining values of these same derivatives at zero lift are inadequate at transonic speeds.

These abstract cards are inserted in Technical Reports for the convenience of Librarians and others who need to maintain an Information Index.

Cut here

ARC CP No.1310
May 1973

Ross, A. Jean
Edwards, Geraldine F.
Waterfall, A. P.

533.693.3 :
533.695.16 .
533.6.013.417 :
533.6.013.601

THE DYNAMIC STABILITY DERIVATIVES OF A SLENDER WING AT ZERO AND MODERATE LIFT, A COMPARISON OF THEORY WITH FREE-FLIGHT MODEL TESTS, M = 0.8 TO 2.0

The longitudinal and lateral stability derivatives of a slender wing and fin configuration (AGARD 'G' standard model) have been measured at near-zero and at moderate lift using rocket-launched free-flight models. Comparisons are made with theoretical estimates of the derivatives, and with previous experimental results from models flying at near-zero lift. The derivatives showing the greatest dependence on angle of attack are z_w, m_w and ℓ_v. The results also show that the linear theories used for obtaining values of these same derivatives at zero lift are inadequate at transonic speeds.

ARC CP No.1310
May 1973

Ross, A Jean
Edwards, Geraldine F.
Waterfall, A. P.

533.693.3 :
533.695.16 :
533.6.013.417 :
533.6.013.601

THE DYNAMIC STABILITY DERIVATIVES OF A SLENDER WING AT ZERO AND MODERATE LIFT; A COMPARISON OF THEORY WITH FREE-FLIGHT MODEL TESTS, M = 0.8 TO 2.0

The longitudinal and lateral stability derivatives of a slender wing and fin configuration (AGARD 'G' standard model) have been measured at near-zero and at moderate lift using rocket-launched free-flight models. Comparisons are made with theoretical estimates of the derivatives, and with previous experimental results from models flying at near-zero lift. The derivatives showing the greatest dependence on angle of attack are z_w, m_w and ℓ_v. The results also show that the linear theories used for obtaining values of these same derivatives at zero lift are inadequate at transonic speeds.

Cut here

DETACHABLE ABSTRACT CARDS

DETACHABLE ABSTRACT CARDS

1975

Published by
HER MAJESTY'S STATIONERY OFFICE

Government Bookshops
49 High Holborn, London WC1V 6HB
13a Castle Street, Edinburgh EH2 3AR
41 The Hayes, Cardiff CF1 1JW
Brazennose Street, Manchester M60 8AS
Southey House, Wine Street, Bristol BS1 2BQ
258 Broad Street, Birmingham B1 2HE
80 Chichester Street, Belfast BT1 4JY
Government Publications are also available through booksellers

C.P. No. 1310

ISBN 011 470894 0